한국해양공학회지 제19권 제2호, pp 12~18, 2005 (ISSN 1225-0767)

Hindcasting of Storm Surge at Southeast Coast by Typhoon Maemi

HIROYASU KAWAI*, DO-SAM KIM**, YOON-KOO KANG***, TAKASHI TOMITA* AND TETSUYA HIRAISHI*
*Marine Environment and Engineering Department, Port and Airport Research Institute, Yokosuka, Japan
**Civil and Environmental System Engineering, Korea Maritime University, Busan, Korea
***Technology Division, Engineering and Construction Group, Samsung Corporation, Sungnam, Korea

KEY WORDS: Typhoon Maemi, Numerical Model, Storm Surge, Waves, Astronomical Tide

ABSTRACT: *Typhoon Maemi landed on the southeast coast of Korea and caused a severe storm surge in Jinhae Bay and Masan Bay. The tide gage in Masan Port recorded the storm surge of a maximum of more than 2m and the area of more than 700m from the Seo Hang Wharf was flooded by the storm surge. They had not met such an extremely severe storm surge since the opening of the port. Then storm surge was hindcasted with a numerical model. The typhoon pressure was approximated by Myers' empirical model and super gradient wind around the typhoon eye wall was considered in the wind estimation. The land topography surrounding Jinhae Bay and Masan Bay is so complex that the computed wind field was modified with the 3D-MASCON model. The motion of seawater due to the atmospheric forces was simulated using a one-layer model based on non-linear long wave approximation. The Janssen's wave age dependent drag coefficient on the sea surface was calculated in the wave prediction model WAM cycle 4 and the coefficient was inputted to the storm surge model. The result shows that the storm surge hindcasted by the numerical model was in good agreement with the observed one.*

1. INTRODUCTION

Typhoon Maemi in 2003 landed on the southeast coast of Korea where its storm surge, high waves, and astronomical high tide triggered the most severe coastal disaster in Korea since Typhoon Sarah in 1959. In Masan City on Masan Bay, the residential and commercial area of more than 700m from the Seo Hang Wharf was flooded by the storm surge. They had not met the attack of such an extremely sever storm surge since the opening of Masan Port. The tide gage on the northwest coast of the bay recorded the storm surge of a maximum of more than 2m, but the workroom of the tide observation tower was damaged due to the high waves. That is a reason why the hindcasting of the storm surge with a numerical model is essential to verify the tide record and deeply understand what happened in the bay.

2. TYPHOON PRESSURE AND WIND FIELD

Fig. 1 shows the track of Typhoon Maemi. The typhoon passed by the JeJu Island and landed on the southeast coast of Korean Peninsula at 21hr, 12 September 2003 with a central pressure and a progression speed of 950hPa and 45 km/h, respectively. While the typhoon was passing by Jinhae Bay and Masan Bay, the level of the astronomical tide reached near the level of the high tide of a spring tide.

2.1 Typhoon Pressure Field

The typhoon pressure field for the storm surge simulation is often approximated to a concentric circular distribution. The empirical model by Myers and Malkin (1961) is assumed in this paper.

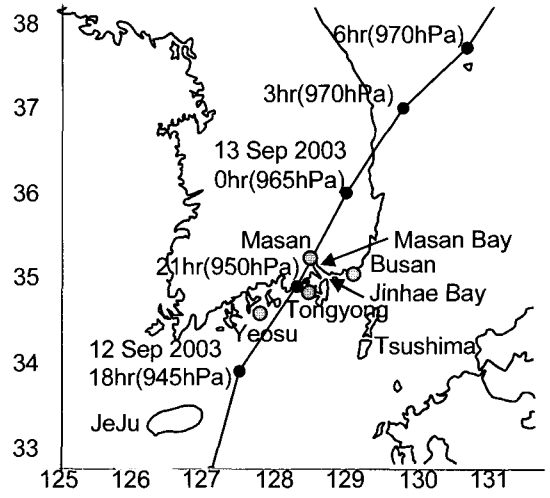

Fig. 1 Track anad central pressure of Typhoon Maemi

제1저자 Kawai 연락처 : 3-1-1, Nagase, Yokosuka 239-0826, Japan
+81-468-44-5052 kawai@pari.go.jp

$$p(r) = p_c + \Delta p \exp\left(-\frac{r}{r_0}\right) \quad (1)$$

where, p_c is the central pressure, Δp is the pressure differential, r is the radial distance from the typhoon center, and r_0 is the radius of maximum wind speed.

The latitude, longitude and central pressure of the typhoon at each hour were issued from Japan Meteorological Agency. The radius of maximum wind speed, r_0, was estimated using the pressure data observed at more than 30 meteorological stations in west Japan and 4 ones in Korea.

Fig. 2 shows the time variation of the pressure at the points near the typhoon track. Their locations are shown in Fig. 1. The typhoon model described by eq. (1) gives the pressure that is in agreement with the observed one.

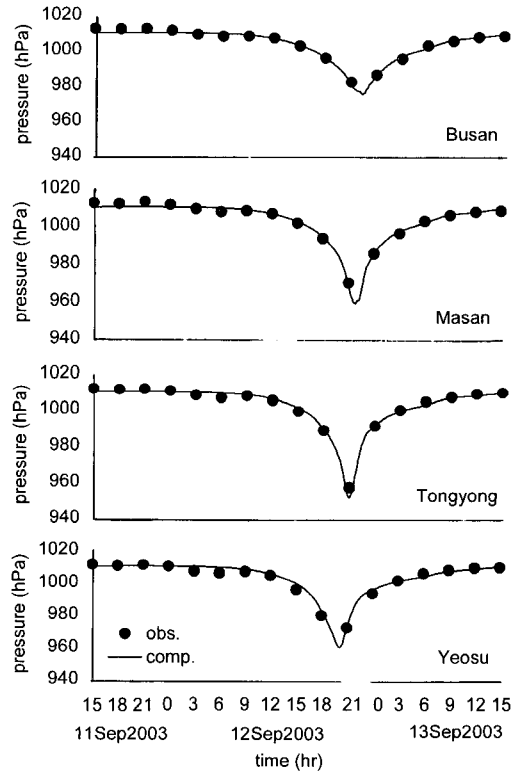

Fig. 2 Time variation of the pressure in Korea

2.2 Typhoon Wind Field

The speed of friction free wind far from the sea surface, U_G, is calculated by

$$U_G = \frac{1}{2}\left\{(fr - V_T \sin\beta)^2 + 4\frac{r}{\rho_a}\frac{\partial p}{\partial r}\right\}^{\frac{1}{2}} + \frac{1}{2}(fr - V_T \sin\beta) \quad (2)$$

where f is Coriolis parameter, V_T is the progression speed of the typhoon, β is the angle which the vector from the typhoon center to the point and the vector of the typhoon progression make, and ρ_a is the density of air. The wind speed on sea surface, namely marine wind speed, W, is given by

$$W = C_1(X) U_G \quad (3)$$

where $X=r/r_0$ is the non-dimensional radial distance from the typhoon center, and $C_1(X)$ is the coefficient for counting reduction of wind speed due to sea surface friction.

As the typhoon passed by Jinhae Bay and Masan Bay, the wind field near the typhoon eye should be exactly reproduced. Then the marine wind speed was estimated with the empirical coefficient (Mitsuta and Fujii, 1987) including the effect of super gradient wind due to typhoon three-dimensional structure.

$$C_1(X) = C_1(\infty) + \{C_1(X_p) - C_1(\infty)\} \cdot \left(\frac{X}{X_p}\right)^{k-1} \exp\left\{\left(1-\frac{1}{k}\right)\left[1-\left(\frac{X}{X_p}\right)^k\right]\right\} \quad (4)$$

where, k is the parameter (=2.5), $C_1(\infty)$ is the coefficient at the remote point from the typhoon center (=2/3), X_p is the distance of maximum coefficient (=0.5), and $C_1(X_p)$ is the maximum value of the coefficient which is empirically determined as

$$C_1(X_p) = \frac{2}{3}\left\{1 + 10^{(0.0231\Delta p - 1.95)}\right\}^{\frac{1}{2}} \quad (5)$$

Such an empirical coefficient has been introduced into the estimation of the marine wind field of Typhoon Bart in 1999 on the coast of the Kyushu Island (Kawai et. al, 2003, 2004).

2.3 Modification of Wind Field by 3D-MASCON Model

The wind field of the empirical typhoon model does not fulfill the atmospheric continuity. Jinhae Bay and Masan Bay are so slender and curved that the effect of the land geographical feature on the wind field should not be neglected. For these reasons, a three-dimensional grid data set of the land topography was made within the whole area shown in Fig. 3. Its dimension is 168 grids (100.8km) and 150 grids (90.0km) in the direction of longitude and latitude, respectively, by 60 grids (altitude: 0 to 1,500 m) in the vertical direction. The vertical grid interval is narrow for low altitude. Initial wind speeds and directions at the grids were assumed using the typhoon model, and then they were modified with the 3D-MASCON model (Goto and Shibaki, 1993) to fulfill the atmospheric continuity with the minimum quantity of their modification.

Fig. 3 compares the modified wind field with the initial one at

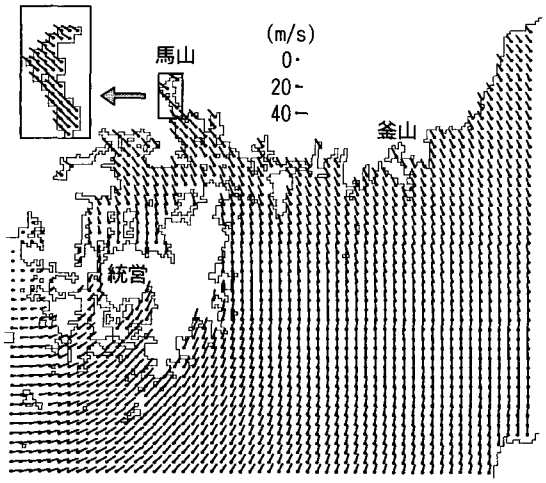

(a) Initial wind field

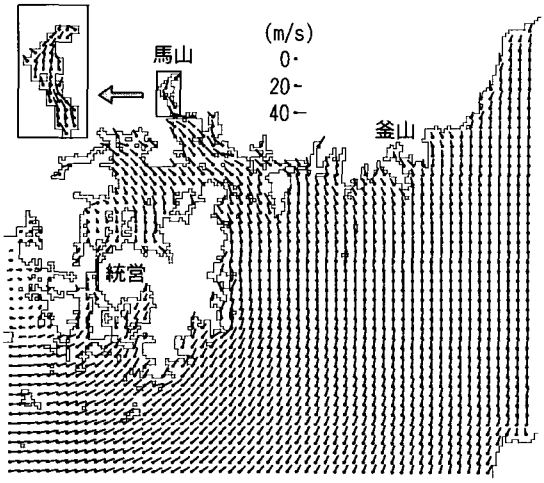

(b) Modified wind field

Fig. 3 Comparison of wind fields

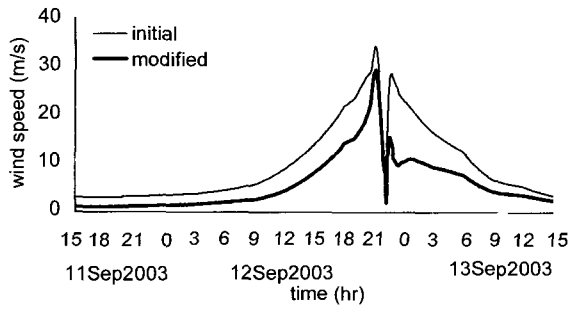

Fig. 4 Time variation of wind speed in Masan Port

21hr, 12 September 2003, when the typhoon center arrived near Tongyong City. The wind flow modified with the 3D-MASCON model seems to be smoothly blowing on the axis of Jinhae Bay and Masan Bay, while the initial wind flow is blowing toward northwest regardless of the land geographical feature.

Fig. 4 shows the time variation of the wind speed in Masan Port. The maximum speed of the initial and modified wind is approximately 34m/s and 29m/s, respectively. The 3D-MASCON model decreased the wind speed especially around the second peak. It means that the speed of the wind blowing from Masan Bay to Daehang Strait at the rearward semicircle of the typhoon was reduced significantly.

3. STORM SURGE

3.1 Governing Equation of the Storm Surge

In this paper, the storm surge was simulated with a one- layer model based on non-linear long wave approximation. Its governing equations are as follows:

$$\frac{d\eta}{dt} + \frac{\partial M}{\partial x} + \frac{\partial N}{\partial y} = 0 \tag{6}$$

$$\frac{\partial M}{\partial t} + \frac{\partial}{\partial x}\left(\frac{M^2}{D}\right) + \frac{\partial}{\partial y}\left(\frac{MN}{D}\right) = fN - gD\frac{\partial \eta}{\partial x} - \frac{D}{\rho_w}\frac{\partial p_0}{\partial x} + \frac{\tau_{sx} - \tau_{bx}}{\rho_w} + A_h\left(\frac{\partial^2 M}{\partial x^2} + \frac{\partial^2 M}{\partial y^2}\right) \tag{7b}$$

$$\frac{\partial N}{\partial t} + \frac{\partial}{\partial x}\left(\frac{MN}{D}\right) + \frac{\partial}{\partial y}\left(\frac{N^2}{D}\right) = -fM - gD\frac{\partial \eta}{\partial y} - \frac{D}{\rho_w}\frac{\partial p_0}{\partial y} + \frac{\tau_{sy} - \tau_{by}}{\rho_w} + A_h\left(\frac{\partial^2 N}{\partial x^2} + \frac{\partial^2 N}{\partial y^2}\right) \tag{7b}$$

where, x and y are the horizontal coordinates, M and N is the flux flow in direction of x and y coordinate, respectively, η is the surface elevation due to the storm surge, D is the total depth (=still water depth + storm surge), A_h is the horizontal kinematic eddy viscosity coefficient, p_0 is the pressure on the sea surface.

The symbol τ_{sx} and τ_{sy} are the tangential stress on sea surface in direction of x and y coordinate, respectively,

$$\tau_{sx} = \rho_a C_D W_x \sqrt{W_x^2 + W_y^2} \tag{8a}$$

$$\tau_{sy} = \rho_a C_D W_y \sqrt{W_x^2 + W_y^2} \tag{8b}$$

where W_x and W_y is the wind speed in direction of x and y coordinate, respectively, and C_D is the drag coefficient on the sea surface. The drag coefficient by Mitsuyasu and Kusaba (1984) is often assumed in storm surge simulations for Japanese bays.

$$C_D = \begin{cases} (1.290 - 0.024W)/10^3 & (W < 8) \\ (0.581 + 0.063W)/10^3 & (W \geq 8) \end{cases} \tag{9}$$

This coefficient is determined by the wind speed W alone, although in fact the coefficient varies with the roughness of

the sea surface due to the wave growth and with the angle between the wave and wind directions. The symbols τ_{bx} and τ_{by} in Eqs. (7a) and (7b) represent the tangential stress on the sea bottom in the direction of x and y coordinate, respectively.

$$\tau_{bx} = \frac{\rho_w g n^2}{D^{7/3}} M\sqrt{M^2+N^2} \tag{10a}$$

$$\tau_{by} = \frac{\rho_w g n^2}{D^{7/3}} N\sqrt{M^2+N^2} \tag{10b}$$

where n is the Manning's roughness parameter.

Fig. 5 shows the domains for the storm surge simulation in this paper. The spatial grid interval is 0.2km in Masan Bay and 0.6km in Jinhae Bay. The tide station in Masan Port locates on the northwest coast of Masan Bay in the domain No.9. The water depth at each grid was read from charts. The time interval of the computation is 3s.

3.2 Storm Surge Hindcasting

Fig. 6 shows the distribution of the maximum storm surge hindcasted by the above-mentioned procedure. The storm surge reached about 0.6m in Busan Port, 1m around the entrance of Jinhae Bay and 1.6m in Masan Bay. One of the major reasons by which the numerical model underestimated the storm surge in Masan Bay was that the variation drag coefficient with the sea state was neglected. In fact, young waves have larger drag coefficients than mature waves (Janssen, 1989). This is a reason why wave generation and propagation was simulated with the cycle 4 of the wave prediction model WAM (The WAMDI Group, 1988) as a third generation ocean wave prediction model with a non-linear wave interaction term. This cycle introduced a wave-age dependent drag coefficient (Janssen, 1989),

$$C_D = \left\{\frac{\kappa}{\ln(L/z_0)}\right\}^2 \tag{11a}$$

$$z_0 = \frac{\alpha\tau}{g\sqrt{1-\frac{\tau_w}{\tau}}} \tag{11b}$$

$$\tau_w = \rho_w \int_\theta \int_f 2\pi f \gamma E(f,\theta)\cos(\theta-\varphi)\,df\,d\theta \tag{11c}$$

where, κ is Kalman constant, L is the height above sea surface (=10m), z_0 is the roughness, α is the parameter, τ is the total stress, τ_w is the stress due to waves, ρ_w is the density of sea water, f is the wave frequency, θ is the wave direction, $E(\ )$ is the wave spectrum, γ is the parameter depending on the wave age and the vertical distribution of the wind, and φ is the wind direction.

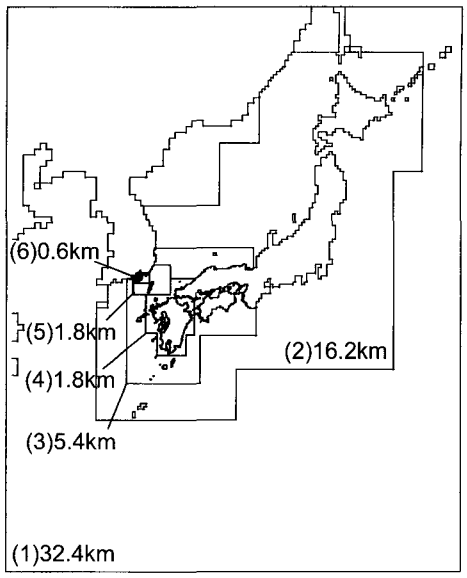

(a) Domains No. 1 to 6

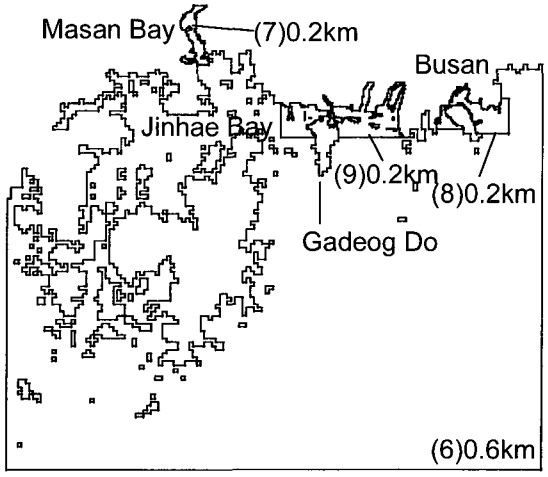

(b) Domains No. 6 to 9

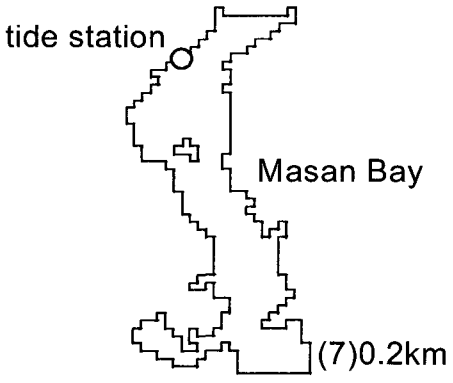

(c) Domain No. 9

Fig. 5 Domains for storm surge simulation

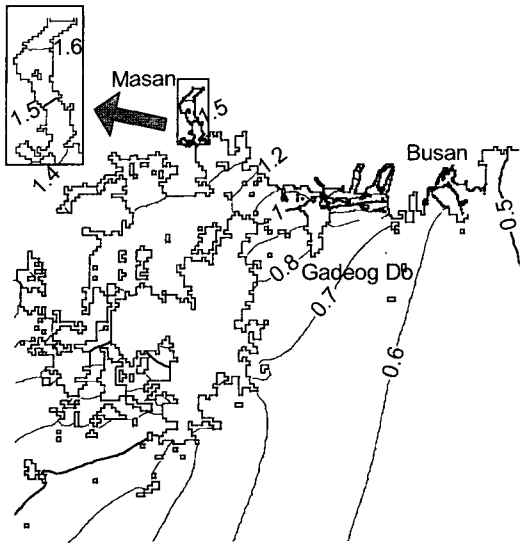

Fig. 6 Distribution of maximum storm surge (drag coefficient by Mitsuyasu and Kusaba)

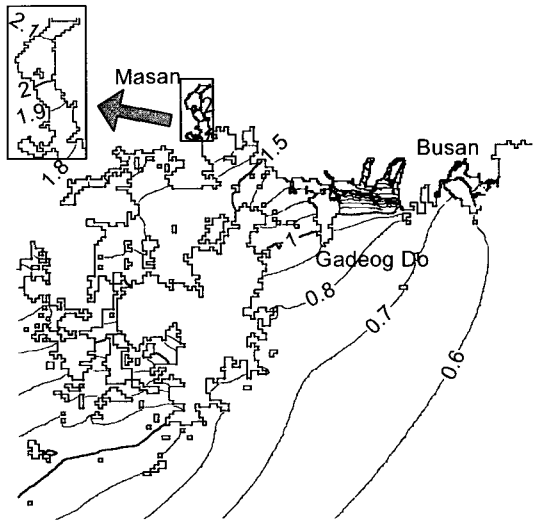

Fig. 7 Distribution of maximum storm surge (drag coefficient by Janssen)

For precise reproduction of the complicated bathymetry of Jinhae Bay and Masan Bay, the spatial grid interval for the wave simulation was set to 0.6km, but the interval was not so fine as the bathymetry contained the breakwaters in Masan Bay. The limiter on the increments in wave energy by Hersbach and Janssen (1999) was introduced in the source term of the wave prediction model.

Fig. 7 shows the maximum storm surge hindcasted with Janssen's drag coefficient. The storm surge reached 2.1m in Masan Bay. Fig. 8 shows the time variation of the storm

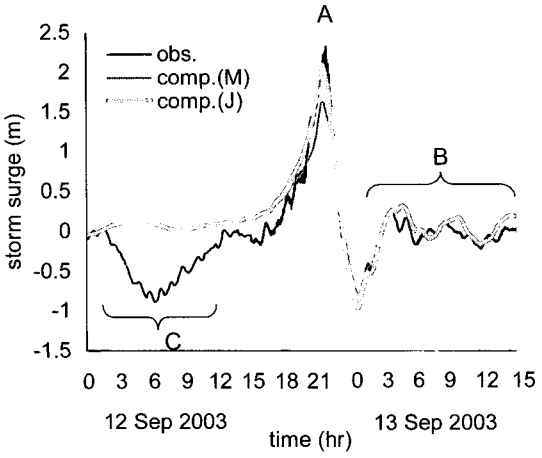

Fig. 8 Time variation of storm surge in Masan Port

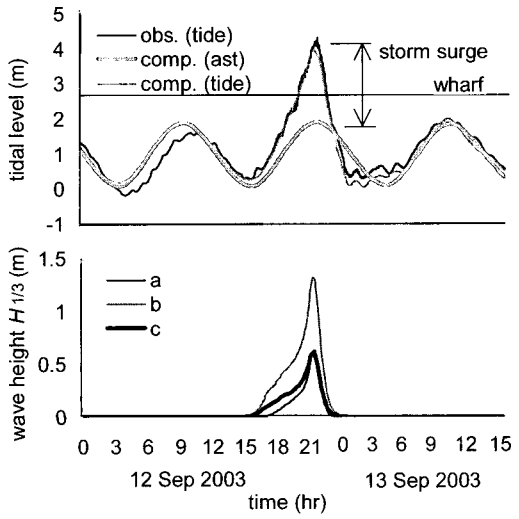

Fig. 9 Time variation of the tidal level and wave height in Masan Port

surge at the tide station in Fig. 5(c). The hindcasted storm surge is in agreement with the observed one, around its peak(A) and resurgence(B) in Fig. 8. It seems that the negative surge(C) in the tide record is not related with the suction effect of depression and wind-drift effect of the typhoon.

The astronomical tide in the domains No. 6 to 9 in Fig. 5 was also computed using the same storm surge model. The astronomical tidal level on the west, south, and east boundaries of the domain No. 6 were computed by the ocean tide prediction system NAO.99b (Matsumoto et al., 2000). The upper graph of Fig. 9 compares the computed astronomical tidal level and the computed tidal level(= computed astronomical tidal level + computed storm surge) with the observed tidal level. The observed tidal level is much lower than the computed one form 4 hr to 11hr, 12

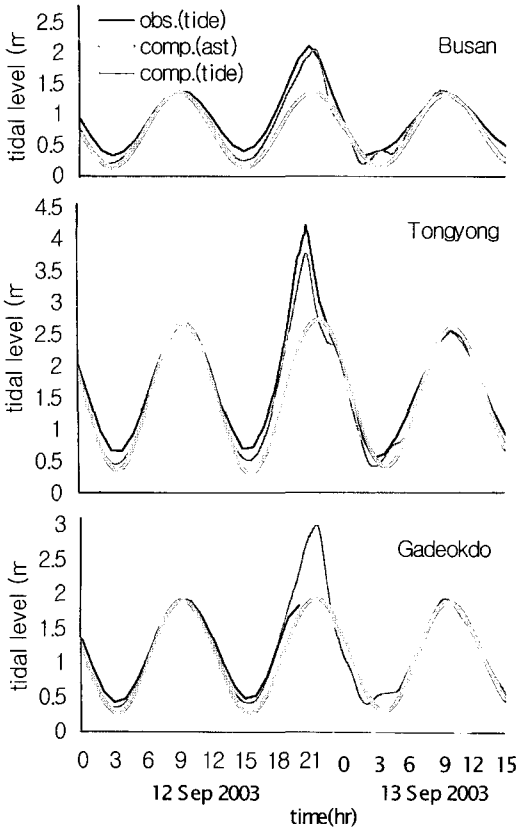

Fig. 10 Time variation of the tidal level at the major points around Masan

September 2003, but its reason is still unknown. Except for that, the computed tidal level gets agree with the observed one.

According to the tide record, the tidal level reached approximately 4.3m above the chart datum level. Since the

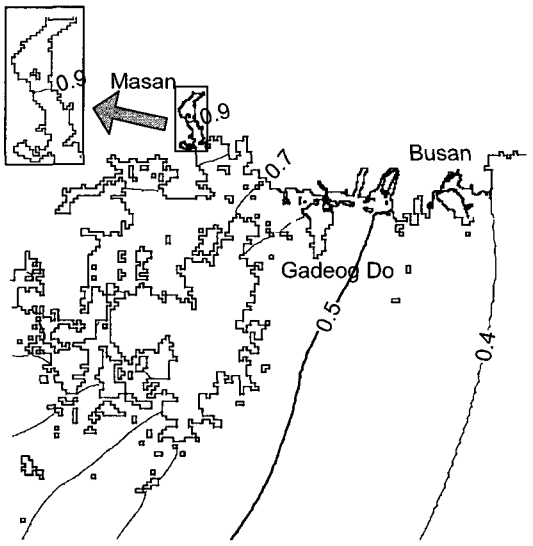

Fig. 11 *Distribution of maximum storm surge due to suction effect*

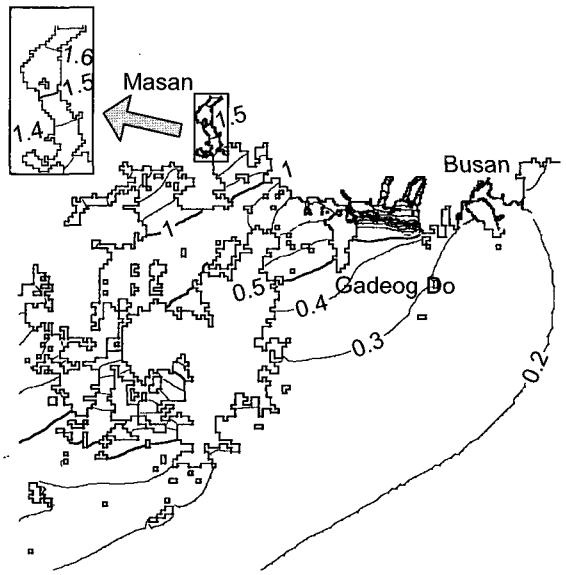

Fig. 12 Distribution of the maximum storm surge due to wind-drift effect

crest height of the Seohang Wharf is about 2.8m, it becomes that the maximum inundation height reached 1.5m at the wharf and 1m or more at the rearward city area. In fact, very clear inundation traces remained on the walls inside and outside of the buildings in the area of within 500m from the wharf. Their heights are between 4.1 and 4.4m, and are near the observed tidal level and the computed one.

The lower graph of Fig. 9 shows the time variation of the significant wave height at the major points in Masan Bay. The maximum significant wave height seemed to be more than 1m around the tide station, point (b) in the figure, and about 0.6m at the north end of the bay, point (a) and Seo Hang Wharf, point (c). The storm surge, astronomical tidal level, and the wave height almost simultaneously reached their maximums.

Fig. 10 compares the computed tidal level with the observed one at the other points. The difference between the computed tidal level and the observed one is small at Busan. The storm surge was underestimated at Tongyong where the bathymetry is very complicated.

3.3 Suction and Wind-Drift Effect

Storm surge is caused by the suction effect of depression and the wind drift effect. Fig. 11 shows the maximum storm surge if only the suction effect acts on the sea surface. The minimum pressure in Masan was approximately 960hPa as shown in Fig. 2. It can be estimated that the suction effect was about 1.7cm/hPa (the storm surge of 0.9m by the depression of 50 hPa). On the other hand, Fig.

12 shows the maximum storm surge if only the wind-drift effect acts on the sea surface. In this case the storm surge reached 1.5m in Masan.

Fig. 13 compares the time variation of (1) the actual storm surge caused by the suction and wind-drift effects, (2) the imaginary one by the suction effect alone, and (3) the imaginary one by the wind-drift effect alone. The maximum value of the actual storm surge is 2.1m. It consists of the suction effect of 0.5m and the wind-drift effect of 1.6m. After the wind-drift effect begins to decrease, the suction

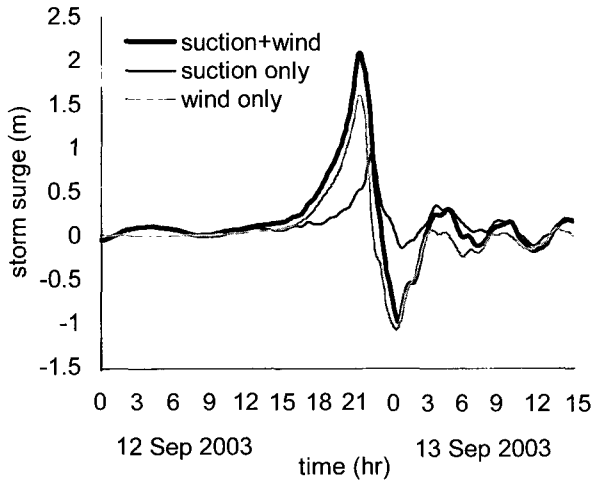

Fig. 13 Time variation of the storm surge in Masan Port

effect reaches the maximum of 0.9m.

4. CONCLUSIONS

The pressure and wind field of Typhoon Maemi were hindcasted by Myers pressure distribution model and the 3D-MASCON model. The storm surge was hindcasted using the one-layer model based on the non-linear long wave approximation with the Janssen's wave age dependent drag coefficient. The result showed that the storm surge by the numerical model was in good agreement with the observed one. It was confirmed that the storm surge exceeded 2m in Masan Bay. However, it is indispensable to investigate carefully why the unrealistic negative surge was included in the tide record. Additionally it is necessary to improve the numerical model to obtain a more accurate result.

ACKNOWLEDGEMENT

We would like to appreciate to many Korean researchers, especially Dr. See-Whan Kang and Dr. Weon-Mu Jeong, Korean Ocean Research & Development Institute, for information and data related with the storm surge disaster and kind assistance of the field investigation in Masan.

REFERENCES

Goto, C. and Shibaki, H. (1993). "A Hindcast of Marine Surface Wind Including Effects of Land Topography", Report of Port and Harbour Research Institute, Vol 32, No 3, pp 65-97.

Hersback, H. and Janssen, PAEM (1999). "Improvement of the Short-Fetch Behavior in the Wave Ocean Model (WAM)" J. of Atmospheric and Oceanic Technology, Vol 16, pp 884-892.

Kawai, H., Kawaguchi, K. and Hashimoto, N. (2003). "Development of a Storm Surge Model Coupled with a Wave Model for Typhoon-caused Wave and Current in a Closed Bay", Report of the Port and Airport Research Institute, Vol 42, No 3, pp 85-110. (in Japanese)

Kawai, H., Kawaguchi, K. and Hashimoto, N. (2004). " Development of Storm Surge Model Coupled with Wave Model and Hindcasting of Storm Waves and Surges Caused by Typhoon 9918", Proceeding of ISOPE 2004.

Janssen, PAEM (1989). "Wave-induced Stress and the Drag of Air Flow over Sea Wave" J. of Physical Oceanography, Vol 19, pp 745-754.

Matsumoto, K., Takanezawa, T. and Ooe, M. (2000). "Ocean Tide Models Developed by Assimilating TOPEX/ POSEIDON Altimeter Data into Hydrodynamical Model: A Global Model and a Regional Model around Japan", J. of Oceanography, Vol 56, pp 567-581.

Mitsuta, Y. and Fujii, T. (1987). "Analysis and Synthesis of Typhoon Wind Pattern over Japan" Bulletin Disaster Prevention Research Institute, Kyoto University, Vol 37, Part 4, No 329, pp 169-185.(in Japanese)

Mitsuyasu, H., and Kusaba, T. (1984). "Drag Coefficient over Water Surface under the Action of Strong Wind" J. of Natural Dias Sci, Vol 6, No 2, pp 43-50.

Myers, V. A., and Malkin, W. (1961). Some Properties of Hurricane Wind Fields as Deduced from Trajectories U.S. Weather Bureau, National Hurricane Research Project, Rept. 49.

The WAMDI Group (1988). "The WAM Model - A Third Generation Ocean Wave Prediction Model" J. of Physical Oceanography, Vol 18, pp 1775-1810.

2004년 11월 18일 원고 접수
2005년 3월 31일 최종 수정본 채택